# Mitigation of ground borne noise in rock railway tunnels—Part I: Track design and simulation

R. Cleave, C. Madshus & L. Grande
*Department of Geomechanics, Norwegian Geotechnical Institute, Oslo, Norway*

Arild Brekke & Karin Rothschild
*Brekke & Strand akustikk as, Oslo, Norway*

ABSTRACT: Railway traffic in shallow depth rock tunnels can give unacceptable levels of ground borne noise in buildings above the tunnel. For such a tunnel under construction in Norway a project involving full scale testing was commissioned by the Norwegian Rail Administration (JBV), with the aim of designing the most cost effective track that satisfied the prescribed residential sound levels. Evaluation of various track designs was based upon the results of a numerical model of the wagon-track-tunnel system. This model and the corresponding input parameters are the focus of this first part of a two part paper; the second part concentrates on the full scale tests. The numerical model presented herein is a one dimensional model of the suspended railcar, rail, sleeper, railway substructure (ballast, ballast mats and backfill) and tunnel floor. The model comprises mechanical mass-spring-damper elements and "geolayer" elements embodied by the one dimensional wave equation. Verification against results from other contributors is presented, and the model is shown to give high quality results with a modicum of computation. The properties of the constituent track materials are also discussed in this paper, with particular attention paid to the in-situ stress conditions.

KEYWORDS: Structure-borne noise, vibration, rail tunnels.

## 1 INTRODUCTION

An example of a shallow depth tunnel under a residential area is shown in Figure 1(a). The section under consideration in this work has an overburden of approximately 5 m, and along this section an extra 1.6 m of rock was blasted from the tunnel floor. In addition to the normal 0.6 m of ballast this results in a total of 2.2 m (between the bottom of the sleeper and the tunnel floor) available for the design and testing of improved track substructure solutions. The main design goals are low cost and high attenuation of the vibrations caused by the train traffic. The design model described herein is a one dimensional model of the suspended railcar, the unsuspended rolling mass of the bogie or axle, the track superstructure (rail, rail pads and sleeper), track substructure (ballast, ballast mats and backfill), and the tunnel floor, as sketched in Figure 1(b). The conical shape of the model is introduced to simulate the spreading of the dynamic load throughout the layers of the substructure. The model itself is made up of linear mass-spring-damper systems, solutions to the one dimensional wave equation, simple

springs and an impedance function relating the force exerted on the rock floor by the lowest substructure layer to the particle velocity of the rock floor. The solution of the model is based

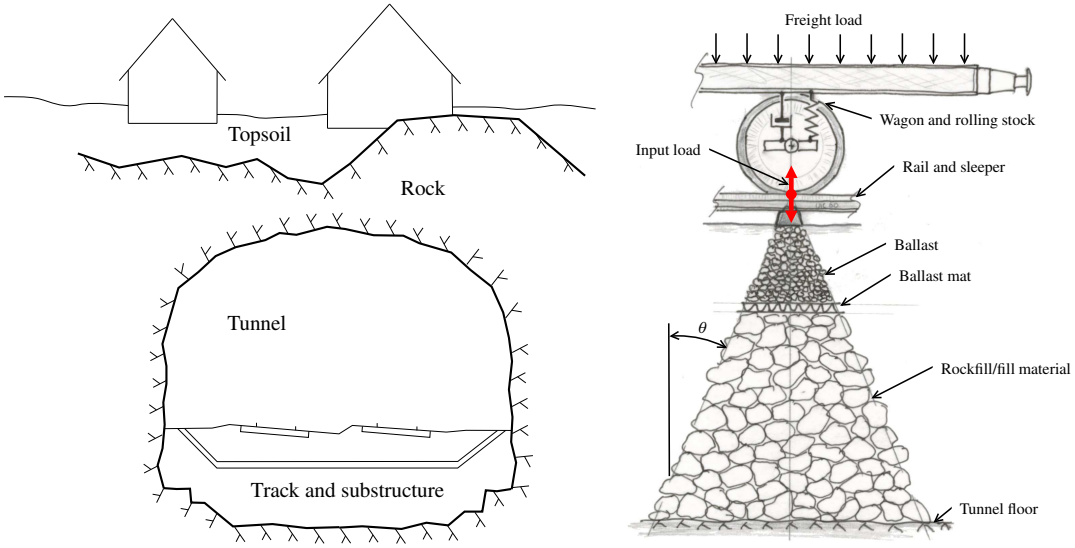


(a) Shallow rail tunnel in residential area.

(b) One dimensional solution of wagon and railway structure.

Figure 1: Problem description.

in the frequency domain, over a frequency range of 20 to 315 Hz. The input to the model is forced excitation of either the unsprung rolling mass (in the case of a single axle freight wagon this means excitation of the axle itself), or of both the unsprung mass and the rail (to model track irregularities and/or out of round wheels).

## 2 MODELLING

Free body diagrams of the parts of the model of Figure 1(b) are shown in Figure 2. The thin ballast mats are modelled by the simple mass-spring-dampers (Figure 2(a)), the substructure layers by the geolayers (Figure 2(c)), and the wagon, rail and sleeper assembly by a mixture of the mass-spring-damper systems (Figure 2(a) and 2(b)). For each component (or layer) the load and displacement for the upper and lower component (or layer) interfaces are shown, where $q$ denotes the interface load and $u$ denotes the interface displacement. The solutions for each component are given below in the frequency domain (uppercase letters are used to denote the frequency domain equivalent of a time domain variable).

Each mass-spring-damper system (Figure 2(a)) is modelled by

$$\begin{bmatrix} {}^1Q_i \\ {}^2Q_i \end{bmatrix} = \frac{k_i}{2k_i - m_i\omega^2} \begin{bmatrix} k_i - m_i\omega^2 & -k_i \\ -k_i & k_i - m_i\omega^2 \end{bmatrix} \begin{bmatrix} {}^1U_i \\ {}^2U_i \end{bmatrix}, \tag{1}$$

where $\omega$ is angular frequency, while the simpler system in Figure 2(b) is modelled by

$$\begin{bmatrix} {}^1Q_i \\ {}^2Q_i \end{bmatrix} = \begin{bmatrix} k_i - m_i\omega^2 & -k_i \\ -k_i & k_i \end{bmatrix} \begin{bmatrix} {}^1U_i \\ {}^2U_i \end{bmatrix}. \tag{2}$$

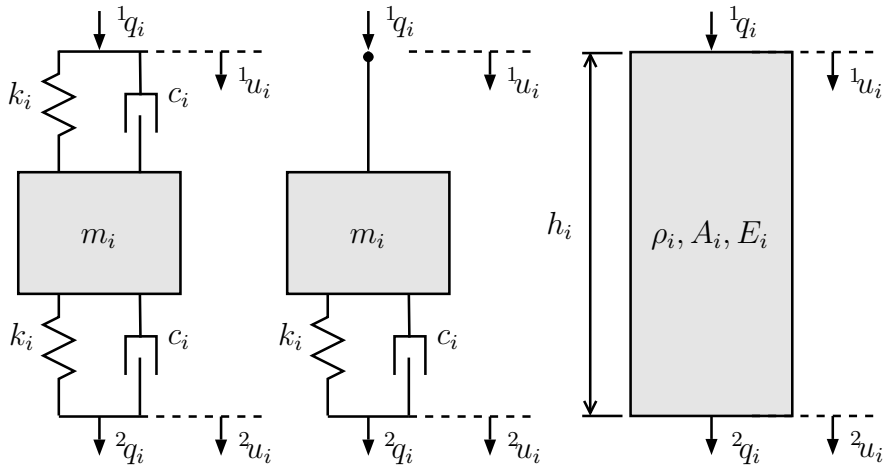


(a) MSD system. (b) Simple MSD system. (c) "Geolayer".

Figure 2: Mechanical and geomechanical components comprising the one dimensional model.

Each "geolayer" is modelled using the one dimensional wave equation, giving

$$\begin{bmatrix} {}^1Q_i \\ {}^2Q_i \end{bmatrix} = \frac{\omega E_i A_i}{C_i} \begin{bmatrix} \frac{1}{\tan\left(\frac{\omega}{C_i}h_i\right)} & -\frac{1}{\sin\left(\frac{\omega}{C_i}h_i\right)} \\ -\frac{1}{\sin\left(\frac{\omega}{C_i}h_i\right)} & \frac{1}{\tan\left(\frac{\omega}{C_i}h_i\right)} \end{bmatrix} \begin{bmatrix} {}^1U_i \\ {}^2U_i \end{bmatrix}, \tag{3}$$

where $C_i$ is the compressional wave speed in the material, $E_i$ is the Young's modulus and $\rho_i$ is the mass density. $A_i$ is the effective cross sectional area of the layer, and is calculated using the load spreading illustrated in Figure 1(b). In the above equations hysteretic damping is introduced using complex-valued stiffnesses and Young's moduli.

Assuming the general form of the above equations ((1)-(3)) to be

$$\begin{bmatrix} {}^1Q_i \\ {}^2Q_i \end{bmatrix} = \begin{bmatrix} K_{i_{11}} & K_{i_{12}} \\ K_{i_{21}} & K_{i_{22}} \end{bmatrix} \begin{bmatrix} {}^1U_i \\ {}^2U_i \end{bmatrix}, \tag{4}$$

then the entire system shown in Figure 1(b) can be combined by satisfying equilibrium and kinematic compatibility, such that

$$\mathbf{Q} = \left[\begin{array}{ccccc|c} K_{1_{11}} & K_{1_{12}} & 0 & \dots & 0 & 0 \\ K_{1_{21}} & K_{1_{22}}+K_{2_{11}} & K_{2_{12}} & \dots & 0 & 0 \\ 0 & K_{2_{21}} & K_{2_{22}}+K_{3_{11}} & \dots & 0 & 0 \\ \vdots & \vdots & \vdots & \ddots & K_{N-1_{12}} & 0 \\ 0 & 0 & 0 & K_{N-1_{21}} & K_{N-1_{22}}+K_{N_{11}} & K_{N_{12}} \\ \hline 0 & 0 & 0 & 0 & K_{N_{21}} & K_{N_{22}} \end{array}\right] \mathbf{U}, \tag{5}$$

or, with the same partitioning:

$$\left[\begin{array}{c} \mathbf{Q}_{\text{known}} \\ \hline \mathbf{Q}_{\text{rock}} \end{array}\right] = \underbrace{\left[\begin{array}{c|c} \mathbf{K}_{11} & \mathbf{K}_{12} \\ \hline \mathbf{K}_{21} & \mathbf{K}_{22} \end{array}\right]}_{\mathbf{K}} \left[\begin{array}{c} \mathbf{U}_{\text{unknown}} \\ \hline \mathbf{U}_{\text{rock}} \end{array}\right]. \tag{6}$$

Here $\mathbf{Q} = [{}^1Q_1, {}^2Q_1 + {}^1Q_2, \dots, {}^2Q_N]^T$ and $\mathbf{U} = [U_1, U_2, \dots, U_N]^T$, where $(U_i = {}^2U_i = {}^1U_{i+1})$. The external load vector $\mathbf{Q}$ is known for every layer interface except

for the interface between the last layer and the tunnel floor[1]. The displacement of the tunnel floor, and thus $U_N$, is assumed to be negligible in comparison to the displacement of the intermediate layer interfaces. This allows for the partitioning shown in (5) and (6), so that the equation $\mathbf{Q}_{\text{known}} = \mathbf{K}_{11}\mathbf{U}_{\text{unknown}}$ in (6) can first be solved for $\mathbf{U}_{\text{unknown}}$, for each frequency in the frequency range of interest. $\mathbf{Q}_{\text{rock}}$ can then be found from the solution to $\mathbf{U}_{\text{unknown}}$.

The interaction between the lowest layer and the rock floor of the tunnel is modelled using the impedance relationship

$$v_t = \frac{Q_N}{\rho_t C_t A_t}, \tag{7}$$

where $C_t$ is the speed of compression waves in the tunnel rock, $A_t$ the area of the effective "footprint" on the floor, $\rho_t$ the mass density of the tunnel rock and $v_t$ the resulting vertical particle velocity of the tunnel floor.

### 2.1 Load spreading

The angle $\theta$ in Figure 1(b) is the spreading angle of the dynamic load from the superstructure, and is assumed constant throughout the track structure. This defines the effective area of each layer, giving $A_i$ in (3) for the geolayers and $k_i$ in (2) for the ballast mats. The area on the top ballast layer is given by the geometry of the sleeper, and the resulting area at the bottom of the substructure is called the "footprint". This footprint is the area over which the dynamic force is distributed from the substructure to the tunnel floor.

### 2.2 Implementation

The solution described above is implemented in MATLAB, with input parameters for the various train and track designs being defined in a spreadsheet. The system of equations in (5) is solved over a frequency range of 10—500 Hz.

## 3 SELECTION OF MATERIAL PARAMETERS

The dynamic stiffness and damping properties of the materials comprising the track substructure have a large effect on the simulation results. Realistic estimation of these input parameters is crucial for the quality of the simulated output. The elastic modulus of the material in each layer is dependent on the instantaneous confining stress, which is in turn dependent on the axle load, depth and compaction. The damping is dependent upon confining stress, load path and frequency. Furthermore, the inhomogeneity and variability inherent in granular materials means that each property is at best an average value.

The granular materials of the substructure have non-linear stress dependent stiffness properties, which lead to a hysteretic behaviour under repeated loading. During the passage of an axle load, the materials undergo a major pseudo static load-deformation cycle with degraded secant stiffness and substantial hysteretic energy loss. The dynamic loads which cause ground borne noise, however, have much lower amplitudes and higher frequencies, and can therefore be considered to be superimposed on the major cyclic loads. Madshus 1997 shows that the response of such materials to the superimposed loads is controlled by the elastic properties of

[1]The known components are either zero (between substructure layers) or an input corresponding to the force from either unbalanced wheels and/or track irregularity/out of round wheels

the material, which is determined by the instantaneous value of the major pseudo static load. In this elastic regime, the stiffness is higher and the damping lower than for the major load cycles.

### 3.1 Elastic modulus of track materials

The work of Duncan et al. 1980 and Madshus et al. 1993 has been used to find the variation of the dynamic Young's modulus for granular materials as a function of confining pressures, and finite element analysis has been used to estimate the confining pressure throughout the track substructure due to normal freight rail loading. From this information the substructure stiffness with respect to depth can be found, as shown in Figure 3. This figure is used to find

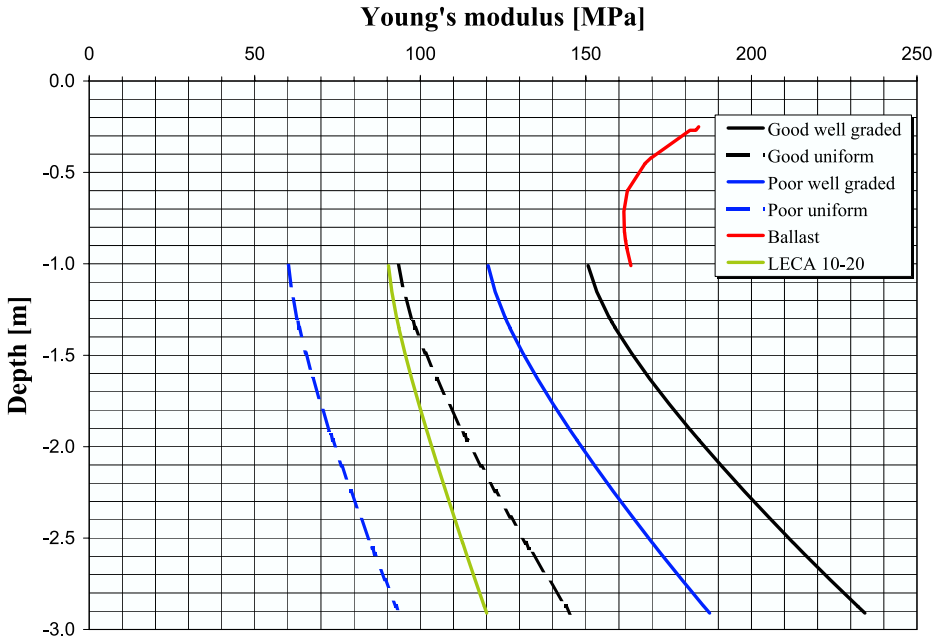


Figure 3: Young's modulus of substructure materials with respect to depth.

the appropriate stiffness for each layer in the model; for example, a 1 m thick ballast may be split into two layers of different stifnesses, according to the average depth of each layer. The various rockfills in Figure 3 differ due to their rock quality (classified here as either "good" or "poor") and uniformity (classified here as either "well graded" or "uniform"). The material LECA (Light Expanded Clay Aggregate) is often used as a fill material where weight is an issue. In the track substructure application this relatively high strength to weight ratio may contribute to the overall vibration attenuation of the substructure, and therefore this material has been included in the design phase.

### 3.2 Damping of track materials

The damping is the materials ability to dissipate vibration energy and reduce resonance vibrations. In the elastic regime, which controls the material behaviour for ground borne noise transmission, the damping is low, typically 2-5%.

Modelling the dynamic response of a track structure with such low material damping leads to sharp dynamic resonances. Because such resonances are not observed in real tracks other mechanisms of damping must exist. One such mechanism is due to non-homogeneity in the

granular layers. Firstly, no layer has a constant, unique thickness, and no layer interface is an ideal flat surface. Secondly, granular materials are internally inhomogeneous, and load bearing occurs along fairly arbitrary chains of particle-to-particle contact forces, as illustrated in Figure 4(a). Dynamically, a layer of granular material can therefore be thought of as an as-

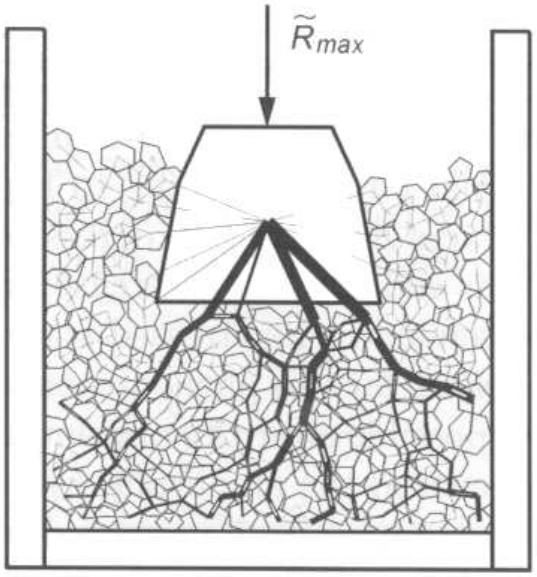


(a) Ballast loading, indicating dissimilar load paths. From Kruse and Popp 2003

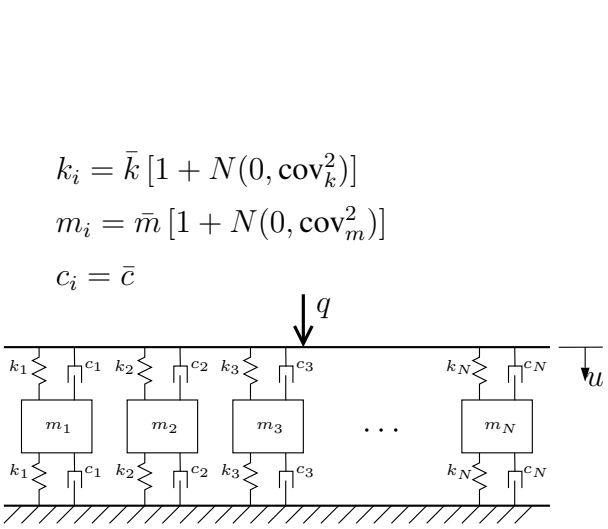


(b) Randomised MSD system.

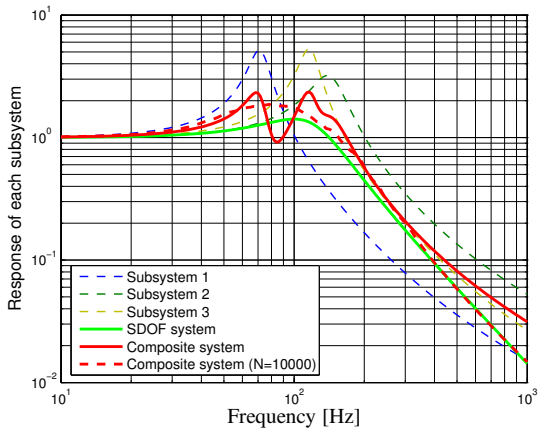


(c) Frequency response of randomised MSD system. The stippled lines indicate the response of each individual MSD system. The comparison SDOF system has 40% damping.

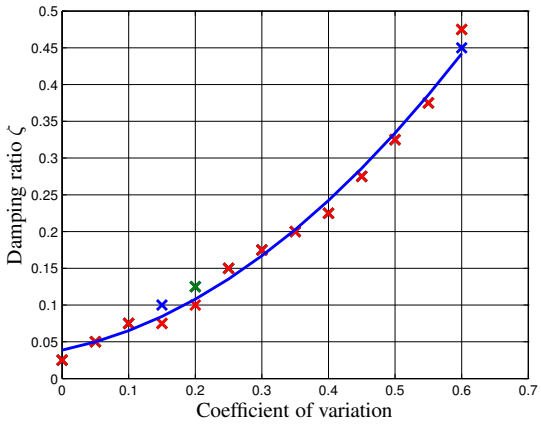


(d) Coefficient of variation vs. damping ratio.

Figure 4: Mechanism and effect of randomised properties

sembly of multiple load bearing members, each with its individual dynamic properties. This effect can be simulated by an assembly of discrete dynamic systems, with randomly distributed properties, as illustrated in Figure 4(b). Figure 4(c) illustrates the behaviour of a granular layer modelled by three individual systems. At frequencies where one of the systems undergoes resonance, and thus high load transfer, it is restrained by the other systems which are not at resonance. To realistically model a granular layer a much larger number of subsystems is needed.

As shown in Figure 4(c), an increase in the number of individual systems results in a frequency response of the composite system that approaches that of the high damping SDOF system. Figure 4(d) plots this apparent equivalent SDOF damping ratio versus the coefficient of variation of the sybsystem parameters. From the figure, and general judgement on the randomness of the load-carrying chains in granular materials, one can conclude that a damping ratio of at least 15% can be justified for a granular layer.

### 3.3 Example simulation

Consider an example of a loaded freight wagon and a tunnel track comprising of track, sleeper, ballast and ballast mat (Table 1). Figure 5(a) plots the accelerations resulting from a dynamic

Table 1: Example parameters.

| | Thickness | Mass | Stiffness | Damping |
|---|---|---|---|---|
| Wagon | | 22500kg | 8MN/m | 10% |
| Unsprung mass | | 1500kg | 395GN/m | 10% |
| Ballast | 0.3m | 2100kg/m$^3$ | 200MPa | 15% |
| Ballast | 0.3m | 2100kg/m$^3$ | 160MPa | 15% |
| Ballast mat | 0.04m | 10kg/m$^3$ | 20MN/m$^3$ | 15% |

force of 1 kN applied to the unsprung mass (which includes here the rails and sleeper). The effect of the ballast mat is shown in Figure 5(b), where the ratio of the force transfer function (from the applied dynamic load to the tunnel floor) of the track without ballast mat over that of the track with ballast mat is plotted. This ratio is known as the "Insertion Loss", and gives a frequency dependent measure of the design.

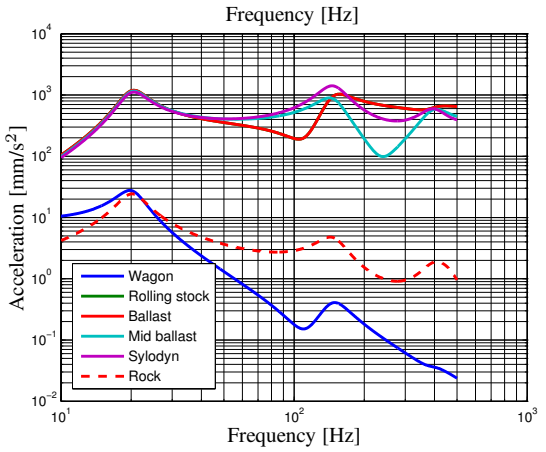


(a) Accelerations at interface of layers/components. (The green curve of the sleeper (this includes the entire unsprung mass) acceleration is covered by the top ballast layer (red curve).)

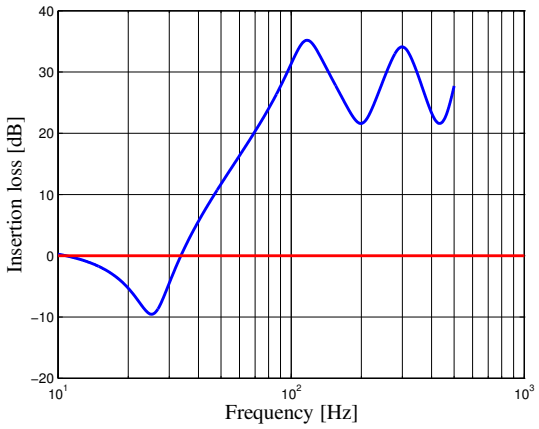


(b) Insertion loss due to the addition of a ballast mat.

Figure 5: Example results for a simple track structure.

### 3.4 Validation

In Wettschureck 1997 a simplified model for structure borne noise for above ground railway lines is compared againt experimental measurements. The results from both the present model and that of Wettschureck are compared in Figure 6. The insertion loss created by the addition of a ballast mat to an otherwise standard ballasted track has been calculated. Up to around 100 Hz

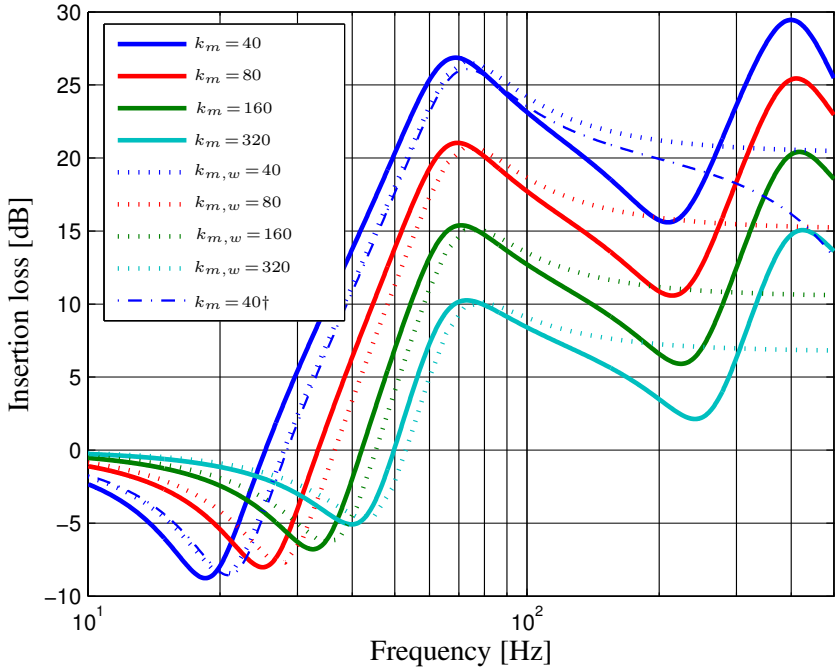


Figure 6: Comparison of the present model (solid lines) with with Figure 7 in Wettschureck 1997 (dotted lines). Units of the ballast stiffness $k$ are MN/m$^3$. †: Insertion loss computed by the present model with a nearly massless ballast.

the two models predict very similar insertion losses, however the troughs and peaks occur at slightly different frequencies. This is because the model in Wettschureck 1997 assumes a massless ballast—a situation which can be simulated using the present model by giving the ballast a very small mass density (see the dash-dot line in Figure 6). At higher frequencies the present model shows the effect of the higher modes of the ballast, which is again not modelled by the method used in Wettschureck 1997.

## 4 SIMULATION OF TRACK SOLUTION FOR FULL SCALE TESTING

The design model was used to compare a raft of design solutions, and, based upon insertion loss and cost, three were chosen for full scale testing. These are described in Table 2, and the insertion loss for each, relative to a standard ballasted track, is shown in Figure 7. The insertion loss (IL) here is calculated according to

$$IL(\omega) = \left| \frac{H_{\text{ref}}(j\omega)}{H(j\omega)} \right|, \tag{8}$$

Table 2: Three solutions chosen for full scale tests.

| | **Alternative 1** | **Alternative 2** | **Alternative 3** |
|---|---|---|---|
| **Axle load** | 22.5kN | 22.5kN | 22.5kN |
| **Rolling mass** | 1200kg | 1200kg | 1200kg |
| **Sleeper** | 300kg | 300kg | 300kg |
| **Ballast** | 0.6m | 0.6mm | 0.6m |
| **Mat** | 85mm, 24MN/m$^3$ | | |
| **Extra fill** | 1.6m poor well-graded fill | 1.6m poor well-graded fill | 0.8m LECA, 0.8m poor well-graded fill |
| **Mat** | | 85mm, 24MN/m$^3$ | 85mm, 24MN/m$^3$ |

where $H_{\text{ref}}(j\omega)$ is the transfer function from the input force to the tunnel floor acceleration for the reference track and $H(j\omega)$ the same transfer function for the track under evaluation. This definition of the insertion loss gives higher values than those shown in Figures 5(b) and 6. The wagon suspension in each case was chosen to produce a 3 Hz natural frequency for the wagon, while the stiffness between the rolling mass and the track models stiff railpads. In addition, to model the real situation better, each track is laid on a 100 mm thick layer of levelling material (this provides a flat working surface on top of the blasted rock floor.

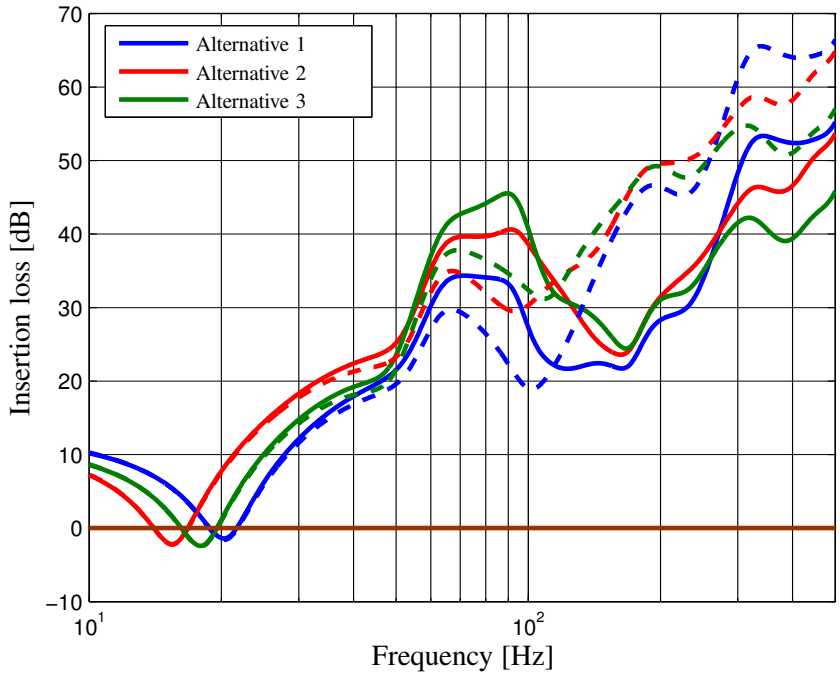


Figure 7: Insertion loss of each of the three proposed track structures, with respect to a standard ballasted track. The solid lines show the insertion loss for an input force at the rail, while the dashed lines indicate the insertion loss for an input excitation at the axle (rolling stock).

## 5 CONCLUSIONS

The track model presented in this paper provides a computationally effective, flexible and easy to use system for simulating the transfer of vibration through a layered railway track. Extensive work has been performed regarding the input parameters for the model (stiffness, density and damping ratios), in order to produce reliable simulations. The model has been applied to various track designs, and used to compare designs based upon the widely used measure of Insertion Loss. Three designs, based upon a standard ballast above layers of rockfill and ballast mats, were chosen for full scale tests. This full scale testing is covered in the companion paper Cleave et al. 2005.

## 6 ACKNOWLEDGEMENTS

The authors would like to thank the Norwegian Rail Administration (JBV) for the funding of this work, and Norconsult AS and Mica AS as for their teamwork and contributions.

## REFERENCES

Augustine, S., Gudehus, G., Huber, G. and Schünemann, A., 2003. *Numerical Model and Laboratory Tests on Settlements of Ballast Track*. In K. Popp and W. Schiehlen, editors, System dynamics and long-term behaviour of railway vehicles, track and subgrade, volume 6 of Lecture notes in applied mechanics, pp. 317–336, Springer-Verlag.

Cleave, R., Madshus, C., Grande, L., Brekke, A. and Rothschild, K., 2005. *Mitigation of ground borne noise in rock railway tunnels - Part II: Full scale tests*. In 7th International Conference on the Bearing Capacity of Roads, Railways and Airfields.

Duncan, J., Byrne, P., Wong, K. and Marby, P., 1980. *Strength, stress-strain and Bulk Modulus Parameters for Finite Element Analysis of Stresses and Movements in Soil Masses*. Technical Report UCB/GT/80-01, Department of Civil Engineering, University of California, Berkeley.

Kruse, H. and Popp, K., 2003. *Model-Based Investigation of the Dynamic Behaviour of Railway Ballast*. In K. Popp and W. Schiehlen, editors, System dynamics and long-term behaviour of railway vehicles, track and subgrade, volume 6 of Lecture notes in applied mechanics, pp. 275–294, Springer-Verlag.

Madshus, C., 1997. *Soil Non-linearity and its Effect on the Dynamic Behaviour of Offshore Platform Foundations*. Ph.D. thesis, Department of Geology, University of Oslo.

Madshus, C., Bessason, B., Stordal, A. and Jenssen, A., 1993. *Dynamic shock wave measuments in coarse saturated rock fill*. In 13th International Symposium on the Military Application of Blast Simulation (MABS 13), pp. 13–17.

Wettschureck, R., 1997. *Measures to reduce structure-borne noise emissions induced by aboveground, open railway lines*. Rail Engineering International, (1):12–16.